CLUSTER 2: Nanoscale Building Blocks

Period: March 16, 2007 to March 15, 2008

Coordinators: Moungi Bawendi and Hongkun Park

Joanna Aizenberg (SEAS, Harvard)
Moungi Bawendi (Chemistry, MIT)
Federico Capasso (SEAS, Harvard)
Kenneth Crozier (SEAS, Harvard)
Cynthia M. Friend (Chemistry & SEAS, Harvard)
Arthur C. Gossard (Materials, UCSB)
Eric Mazur (SEAS, Physics, Harvard)
Hongkun Park (Chemistry, Harvard)
Pierre Petroff (Materials, UCSB)
Shriram Ramanathan (SEAS, Harvard)

International Collaborator(s): Lars Samuelson (Lund University, Sweden)
Seed Funding: Marco Loncar (SEAS, Harvard)

Number of postdoctoral fellows: 3
Number of graduate students: 5
Number of undergraduate students: 3

Introduction

Tremendous progress has been made in the synthesis of nanoscale structures – nanocrystals, nanowires and nanotubes – that serve as building blocks for new devices and applications. However many challenges remain. They include the synthesis of nanostructures with well-defined sizes and shapes, the synthesis of new classes of materials, the in-depth characterization of newly developed nanostructures, the rational organization of these nanostructures into complex functional structures, and the fusion of nanoscale building blocks with state-of-the-art processing techniques, including e-beam lithography and focused-ion-beam sculpting, to build novel devices.

The ***Nanoscale Building Blocks*** cluster conducts a broad multidisciplinary, multi-investigator research program that is designed to address these challenges. The proposed research is built upon the participants' expertise in the synthesis and characterization (both experimental and theoretical) of nanostructured materials. At the core of the program is the ***rational synthesis of new classes of nanostructures that exhibit new size-dependent properties*** that are distinct from bulk materials, with an emphasis on heterostructures and nanostructures with unconventional shape, as well as on zero-, one- and two-dimensional nanostructures made from new materials, including metal chalcogenides. The ***incorporation of nanostructures into novel device geometries*** constitutes another important part. These new devices will be tested to characterize the physical and chemical properties of the building blocks and to evaluate their technological applicability. ***Understanding the behavior of these nanoscale building blocks*** through theoretical investigations is an important part of the effort, because it is essential to advance the scientific and technological frontiers.

Significant Achievements

Material phase transitions have become a promising approach for future electronic and photonic devices:

Hongkun Park is developing new ways to synthesize chalcogenide nanowires. Chalcogenides exhibit a reversible crystalline-amorphous phase change induced by temperature or electric field that is accompanied by dramatic differences in optical reflectivity and electrical resistivity, making these materials promising for optical data storage and phase change random access memory (PRAM). The advantages of PRAM (fast access, low power, low cost, scalable, non volatile) have attracted the electronics industry.

In the last year, Park synthesized single crystalline Sb_2Te_3 nanowires, as well as a radial heterostructure nanowire, composed of an Sb_2Te_3 core and a GeTe shell. The electrical behavior of individual nanowires and nanowire heterostructures confirmed that these nanostructures exhibit the desired memory-switching behavior.

Shriram Ramanathan, supported by a supplement from the Nanoelectronics Research Institute (NRI), is synthesizing high quality VO_2 films and investigating their structural and transport properties for potential use as nanofabricated devices based on phase-transition phenomena. He has demonstrated a conductance transition of ~5 orders of magnitude in a VO_2 film as the temperature was varied near 70 °C. Dramatic changes in the optical reflectance accompany the MI transition.

In a related area, Joanna Aizenberg has developed a new way to the synthesize nanoparticles. She grows them from a droplet of reaction solution floating on top of an array of silicon nanowires that is coated with a superhydrophobic layer. The non-wetting droplet will only be exposed to the nanowire tips, leading to heterogeneous nucleation and localized growth of the material. Aizenberg demonstrated the technique by growing calcium carbonate particles. She is currently exploring the localized deposition of a wide range of materials. For example, the solution can include a range of organic and inorganic compounds that can be deposited from solution. This new approach is promising for a range of applications.

A number of investigators are finding new ways to make photonic systems from nanocrystals, nanowires, and MBE grown structures:

Pierre Petroff is developing a nanostructure called the quantum post that can manipulate confined electrons and holes, and their spins, by using optical pumping. A quantum post is a short quantum wire (~ 20 nm long) with a quantum dot of different material at each end; they are self-assembled during MBE growth. The quantum post acts as an exciton memory device, which can deliver a single photon on demand. An exciton can be stored for tens of millliseconds by dissociating the electron and hole by an applied electric field, preventing recombination. When the field is turned off, the electron and hole rejoin and recombine, emitting a photon. This new device opens new opportunities in photonics.

Federico Capasso is developing efficient nanowire light emitters, for future photonic circuits. He has a new method for mass-fabrication of nanowire photonic and electronic devices: nanowires are placed sideways on a bottom metal contact, a spin-on glass holds them in place, and a second metal contact is deposited on top, patterned with optical lithography. He has used this approach to make UV LEDs from ZnO nanowires.

With Lars Samuelson and electron microscopist David Bell, Capasso is developing optical methods to study the nanowire materials science. They found that twinning in InP nanowires leads to a staggered band alignment between zincblende and wurtzite crystal structures. The twinning introduces a heterojunction inside a chemically homogeneous material allowing one to define a device by controlling twin formation.

Supported by seed funding, Marko Loncar is developing single-photon optical devices, including sources and switches, based on quantum emitters embedded in nanoscale optical cavities. Two types of emitters are considered: Nitrogen vacency (NV) color centers in diamond, and semiconductor nanocrystals. In past year, Loncar developed a way to use focused-ion-beam (FIB) milling and nanomanipulation to make photonic structures from diamond. A photonic crystal cavity for NV centers was fabricated in a diamond membrane. In addition, an array of diamond nanowires was milled in single-crystal CVD synthesized diamond — NV color centers are present inside individual nanowires. For semiconductor nanocrystals, he is embedding nanocrystal quantum dots into photonic crystal cavities made in silicon nitride films. These new fabrication techniques open up new opportunities in photonics.

The Nanoelectronics Research Institute (NRI) was created by the Semiconductor Research Corporation (SRC) to support academic research. The goal is to develop new types of switches for future electronics through the support of academic research. Our Center was selected for an NRI supplement for research in new oxide semiconductors that show promise for switches based on metal-insulator phase transitions. This work is carried out by Shriram Ramanathan, a Harvard faculty member from Intel, and by Venky Narayanamurti. The potential of new devices for the semiconductor industry is evaluated in the Emerging Research Devices (ERD) panel of the International Technology Roadmap Study (ITRS). Robert Westervelt served as part of this panel in 2006, invited by George Bourianoff of Intel.

Synthesis and Characterization of Phase-Change Nanowire Heterostructures

Hongkun Park
Chemistry and Chemical Biology and Physics, Harvard University
Collaborator(s):

Chalcogenides exhibit a reversible crystalline-amorphous phase change induced by temperature or electric field and have been the subject of numerous research activities. Because the phase-change is accompanied by dramatic differences in optical reflectivity and electrical resistivity, these materials can be the basis of data storage media such as CD/DVD and phase-change random access memory (PRAM). In principle, PRAM exhibits many potential advantages over conventional electronic memory, including fast access time, low power consumption, low cost, scalability, and nonvolatility; consequently, the electronics industry has been actively developing and testing PRAM for future nonvolatile memory applications.

The intrinsic properties of chalcogenide materials and their size-dependent variations determine the speed, stability, and miniaturization of PRAM. The most commonly researched chalcogenide glasses contain a combination of Ge, Sb, and Te, sometimes with various dopants. Considerable work has focused on germanium antimony telluride (GST), in particular with a composition $Ge_2Sb_2Te_5$, as a promising compromise between the stable, slowly switching germanium telluride (GeTe) and the less stable, rapidly switching antimony telluride (Sb_2Te_3). The exact mechanism of the phase change in chalcogenide glasses, however, is still under debate, and the evolution of the phase-change properties as the structure's dimensions reach the nanoscale is just beginning to be investigated. Investigating at the nanoscale the extremes of this family, such as Sb_2Te_3 and GeTe, will offer a fuller sense of the chemistry and physics behind these materials.

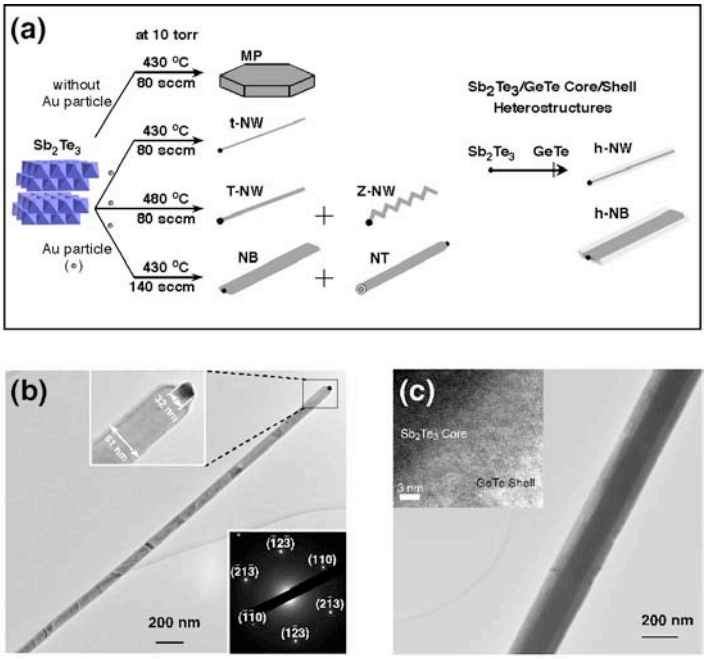

Figure 2.1. (**a**) Morphologies of Sb_2Te_3 nanostructures and Sb_2Te_3 nanowire heterostructures controlled by the growth temperature and the Ar flow rate: MP, microplate; t-NW, thin nanowire (NW); T-NW, thick NW; Z-NW, zigzag NW; NB, nanobelt; NT, nanotube; h-NW, core/shell NW heterostructure; h-NB, core/shell NB heterostructure. (**b**) Transmission electron microscope (TEM) image of a Sb_2Te_3 t-NW. **Top inset**: High-magnification TEM image of the t-NW end with a Sb_xTe_y/Au alloy particle. **Bottom inset**: SAED pattern indexed for rhombohedral Sb_2Te_3. (**c**) TEM image of a core/shell NW showing the uniform GeTe shell coating the Sb_2Te_3 core. **Inset**: high-resolution TEM image of a Sb_2Te_3/GeTe core/shell NW.

In the grant period January 2007-January 2008, we developed a new method to synthesize single-crystalline Sb_2Te_3 nanowires as well as radial heterostructures composed of an Sb_2Te_3 core and a germanium telluride GeTe shell. We also characterized these nanowires and nanowire heterostructures using advanced analytical techniques and electrical measurements. The synthesis employs Au-catalyst-assisted vapor-liquid-solid (VLS) and vapor-solid (VS) mechanisms. Energy-dispersive X-ray spectrometry indicates that Sb and Ge are localized in the Sb_2Te_3 and GeTe portions, respectively, confirming the alloy-free composition in the core/shell heterostructures. Transmission electron microscopy and diffraction studies show that Sb_2Te_3 and GeTe regions exhibit rhombohedral crystal structure. Both Sb_2Te_3 and GeTe grow along the [110] direction with an epitaxial interface between them. We also characterized the electrical behaviors of individual nanowires and nanowire heterostructures, and confirmed that these nanostructures exhibit memory-switching behavior.

Magnetic and Semiconducting Nanoparticle Systems: Properties and Devices

Mounge G. Bawendi
Chemistry, Massachusetts Institute of Technology
Collaborators: Marc A. Kastner (MIT), George M. Whitesides (Harvard), Robert M. Westervelt (Harvard)

The goal of the research is to use novel nanoparticles, synthesized within the project, in devices that (1) probe the photophysics and transport properties of heterostructures based on the nanoparticles, or (2) use the nanoparticles as building blocks for the design of new optical and electronic devices. We describe here four projects: (1) The characterization of cobalt/cobalt oxide magnetic nanoparticles as a model for coupled ferromagnetic/antiferromagnetic nanoparticle systems, (2) transport properties of CdTe quantum dots in device structures, (3) the synthesis of CdSe/CdTe "nanobarbells" that are designed for efficient carrier separation in photodetectors or solar cells, and (4) the design of layered nanocrystal assemblies for funneling carriers towards electrodes for potential solar energy conversion application.

(1) Magnetic nanoparticle systems and their incorporation into optical structures have been the subject of collaboration between Bawendi and Westervelt. Previous accomplishments described the synthesis of nanospheres containing both magnetic iron oxide nanoparticles and fluorescent CdSe/ZnS quantum dots. These magnetic/ fluorescent nanospheres could be manipulated using the nanomagnetic manipulator circuits designed by the Westervelt group. While this work is still ongoing, here we focus on a careful characterization of Cobalt/Cobalt oxide ferro-magnetic/antiferromagnetic core/shell nano-particles which arose out of our work on designing magnetic/fluorescent particle systems. We found that defects associated with the CoO dominated much of the magnetic behavior of this coupled system. We found that the defect moments freeze at low temperature and have a distribution of melting temperatures. These defects stabilize the magnetic Co core through exchange biasing far above the usual blocking temperature. We also found that switching the biasing field at intermediate temperatures during cooling induced a thermal memory effect, illustrated in Figure 2.2, and an opportunity for encoding information.

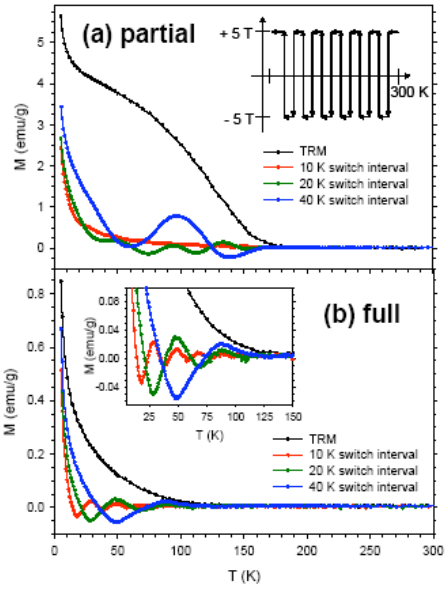

Figure 2.2. Magnetization of partially and fully oxidized Co/CoO nanoparticles after cooling from 300 K while switching the magnetic field back and forth at various intervals.

(2) In an ongoing collaboration between Kastner and Bawendi, we analyzed the details of conduction through nanocrystals of CdTe. We measured the conductance of

close-packed films of CdTe nanocrystals in field-effect structures in the dark and in the presence of light. We found that the majority carriers are holes, that they are injected from gold electrodes into the CdTe nanocrystal films, and that the hole density can be modulated with gate voltage. Secondary photocurrents were found to have a photoconductive gain of ~10 at 10^6 V/cm showing that the hole mobility is higher than the electron mobility. We showed that a single phenomenological description of the field dependence of the hole mobility can explain the dependence of current on source-drain voltage for both dark and light currents.

(3) In our goal of designing and synthesizing nanoheterostructures using wet chemical methods, we demonstrated the synthesis of "nanobarbells" consisting of a CdSe nanorod with a CdTe nanocrystal attached at each end (Fig. 2.3). This system is interesting for its electronic structure because it is an example of a nanoheterostructures that forms a "type II" system, where an exciton undergoes a fast ionization, with the electron preferring the "bar", and the hole preferring the balls at the tips. This rapid intrinsic carrier separation process is essential to high efficiency nanocrystal based potential solar energy devices. It is the first step in the process of extracting the electron and hole at separate electrodes. We are now in the process of testing the conductive and photoconductive properties of devices based on these nanobarbells to understand their basic transport physics, and how their properties could be used in a solar energy conversion scheme.

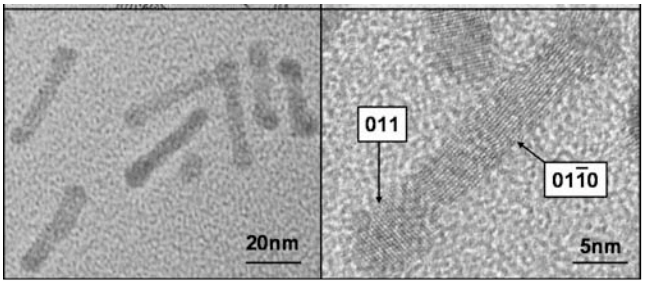

Figure 2.3. TEM images of CdSe/CdTe nanobarbells, designed for fast exciton dissociation.

(4) Students from Bawendi's group have been collaborating with the Whitesides group in designing and characterizing layered nanocrystal structures that are engineered to funnel carriers to the right electrodes in potential solar cell applications. The basic idea is to create a stacked device consisting of an ITO electrode on top of which a series of layers of nanocrystals is deposited, with each layer consisting of smaller particles, and hence with bigger band gaps. By proper choice of the top electrode, directionality is therefore introduced into the device, with the electrons flowing to the ITO, and the holes to the top electrode.

Localized Materials Deposition on a Superhydrophobic Nanowire Array

Joanna Aizenberg
Chemical Engineering, Harvard University
Collaborators: David R. Nelson, George M. Whitesides (Harvard University); Linus A. Fetter (Bell Labs/Alcatel-Lucent Technologies)

One-dimensional nanoscale structures, such as nanowires or fibers, have significant scientific and technological applications for electronic conduction, switching, biological sensors, functional "barcode" designs, self-organization and optics. In a variety of these applications, it is desirable to fabricate an asymmetric fiber that displays different materials at different locations.

The goal of this project is to develop a novel approach for the fabrication of asymmetric nanowire (NW) arrays, in which a guest material is deposited only at one end of each nanowire. Our approach is based on using the superhydrophobic character of an array of NW. A non-wetting droplet of a reaction solution will only be exposed to the tips of the NW leading to a heterogeneous nucleation and subsequent localized growth of materials at one end of the nanostructures. We believe that this approach could be used as a tool for the design of new, functional NW structures.

We have fabricated arrays of NW in Si by deep reactive ion etching (DRIE). The structures were fluorinated by CVD to ensure superhydrophobicity, with contact angles > 150° (Fig. 2.4a). Figure 2.4b shows a non-wetting droplet on a NW substrate, which could be fed independently by multiple microtubing to provide reactant solutions from electronically-controlled syringe pumps. The substrate could be moved relative to the droplet using a stepper-motor controlled microscope stage. Figure 1c shows the footprint of the droplet that outlines the area where precipitation occurred.

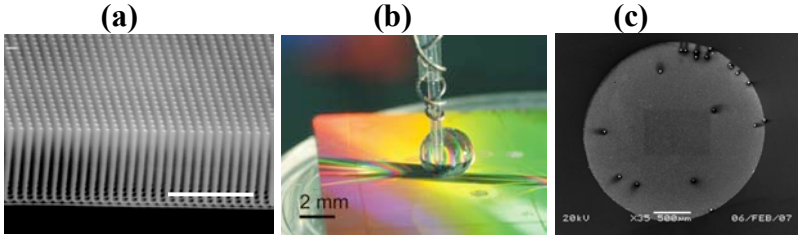

Figure 2.4. (**a**) Si nanowire array. (**b**) Droplet of an aqueous precipitation solution. (**c**) Footprint of the droplet showing the outline of the deposited area.

Figure 2.5 shows our preliminary results of calcium carbonate precipitation. Highly-uniform deposition of particles at the tips of the NW array occurs. By varying the deposition conditions, concentration of ions in the reaction droplet, temperature, deposition time, etc., one can precisely control the size of the particles. Our results provide an indication that this new technique can be used to control the size, shape, and crystallographic orientation of the deposited material. To achieve this, different surface functionalization of NW is used,

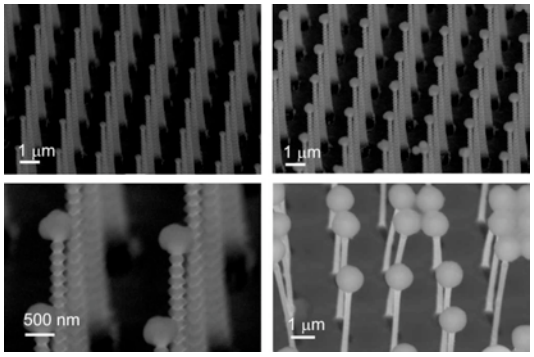

Figure 2.5. Highly uniform precipitates of calcium carbonate form at the tips of the NW array.

to further influence the interaction at the NW liquid interface and to affect the nucleation and growth reactions. When a non-covalent interaction between the NW and the deposited material is used, the deposited particles can be easily removed from the NW tips, and uniform colloidal particles can be collected (Fig. 2.6). Alternatively, when the tips of the NW are selectively functionalized to covalently bond the deposited material, the NW with the firmly attached particles could be shaved off the substrate to produce uniform NW "matches."

We are currently exploring the possibilities of the localized deposition of a wide range of materials on the surfaces of the raised or rough structures exposed to the liquid. For example, the solution can include a range of organic and inorganic compounds that can be deposited from solution. The functionalized raised structure tips can serve as a heterogeneous catalyst for the nucleation and precipitation of the material, or the adsorption of molecules on a surface. The fluid can contain a colloidal suspension of particles or biological cells that can be deposited on the wetted tips of the structured surface, through covalent or non-covalent attachment. The solution can contain a monomer, which is polymerized in the fluid and which is deposited as a polymer on the exposed surfaces of the raised structured surface.

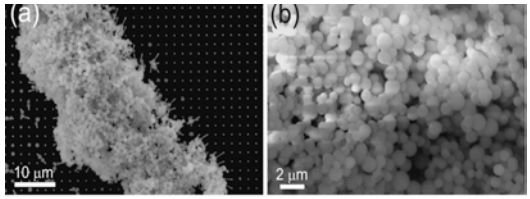

Figure 2.6. Removal of deposited particles.

The surface tension of the liquid and the Young's modulus and geometry of the nanowire array can be regulated and balanced in such a way that the force applied by the liquid will induce bending and clustering of the nanowires into groups. In collaboration with Nelson, we have used a spring approximation theory to build a phase diagram of the deposition process that describes the formation of clusters with varying pattern and size. Based on this approach, we can now rationally design substrates and use conditions (such as the aspect ratio of the posts, pitch spacing between posts, diameter of the deposited particles and the surface tension) that would uniquely lead to the clustering of 2, 3, 4 or more adherent particles (Fig. 2.7). These clusters will then be glued together by the deposited material and form arrays of highly-uniform dimers, tetramers, etc. We are now exploring the ways of removing these complex particles from the NW array and their use in colloidal science. The theoretical analysis of the large-area ordered assembly process induced by the deposition is underway.

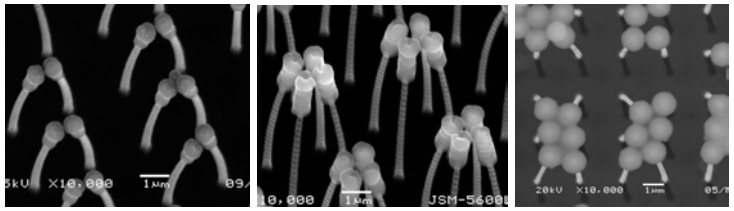
Figure 2.7. NW clustering and the formation of particle dimers, tetramers, etc.

We believe that our approach will result in the development of a new fabrication strategy, which will lead to highly uniform arrays of precipitate deposits grown locally onto nanoscale fibers, in a rapid, room-temperature process. The method could be applied quite generally to a wide range of nucleation/growth precipitation reactions producing novel functionalized asymmetric nanowire arrays and 3-D nanostructure.

Nanowire Photonics: Light-Emitting Diodes and New Heterostructures

Federico Capasso
Applied Physics and Electrical Engineering, Harvard University
Collaborators: Kenneth B. Crozier, Vinothan Manoharan, George M. Whitesides (Harvard University); Lars Samuelson (Lund University)

Research Goal, Approach and Accomplishments. During the last year, Capasso and his group have continued a nanowire optoelectronics program with the goal of developing efficient, room-temperature, electrically-pumped nanowire light emitters, which could form the basis for future integrated photonic circuits. After having achieved significant understanding of the physics underlying the operation of such devices, they have developed a powerful new method for *the mass-fabrication of nanowire photonic and electronic devices*. Their technique is based on spin-on glass technology and the photolithographic definition of independent electrical contacts to the top and bottom of a nanowire. This method can be used on nanowires of any semiconductor type and is completely scalable since every step can be performed over an entire wafer. They have demonstrated this method by fabricating ultraviolet (UV) nanowire light-emitting diodes (LEDs) using ZnO nanowires.

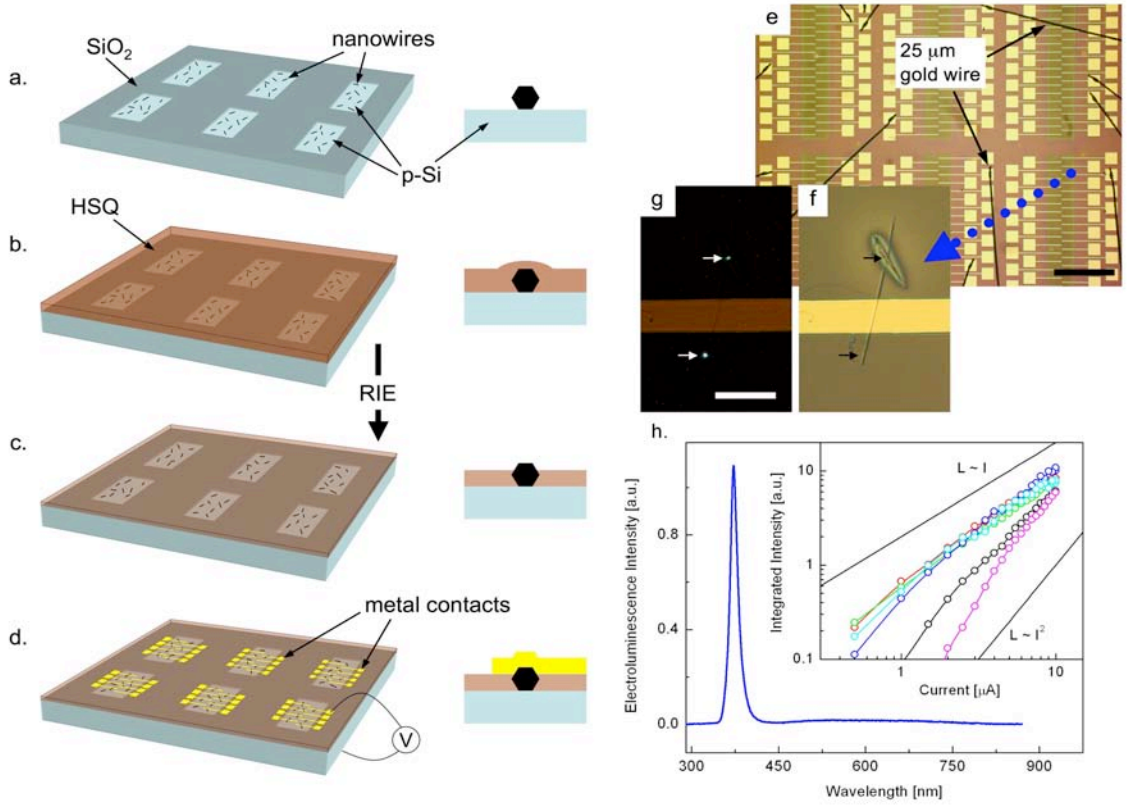

Figure 2.8. Scalable fabrication of nanowire photonic and electronic circuits using spin-on glass. (**a-d**) Schematic illustration of the key steps for the fabrication of p(substrate)-n(nanowire) heterojunction diodes, including (**a**) deposition of nanowires over the substrate, (**b**) spin-coating of HSQ (spin-on glass), (**c**) reactive ion etch of HSQ, and (**d**) deposition of a periodic metal electrode array using photolithography. The figures on the right show a detail of the process for an individual nanowire in cross section, whereas the figures in the left show an overall view of the procedure, emphasizing its scalability and parallelism. (**e-g**) Optical micrographs of p-Si/SiO_2/n-ZnO heterojunction LEDs: (**e**) is an optical micrograph of an

finished wafer (scale bar is 1 mm), and (**f**) is a zoomed-in micrograph of a single-nanowire UV LED. (**g**) shows the same device under a forward bias exhibiting light emission, indicated by the arrows. The scale bar is 30 mm. (**h**) Room-temperature electroluminescence spectra from a ZnO nanowire LED. The inset shows the current dependence of the light intensity for six different devices, which emphasizes the reproducibility of the method.

The Capasso group has also initiated a program exploring the optical properties of novel nanowire materials. In the past year, in collaboration with Dr. David Bell of the Center for Nanoscale Systems (CNS) at Harvard, they have experimentally observed the effect of rotation twinning on the optical properties of zinc blende (ZB) indium phosphide (InP) nanowires. In order to establish the correlation between the observed optical properties with the twinning structure, they have developed a new type of substrate that has made it possible to perform high excitation power photoluminescence (PL) and transmission electron microscopy (TEM) on the same nanowire. Using this technique, they have observed a different PL behavior for rotation twinned InP nanowires compared with single crystal ZB InP nanowires. These observations were qualitatively explained based on the staggered band alignment between ZB- and wurtzite (WZ)-InP. These findings support early theoretical studies that rotation twinning introduces a heterojunction in a chemically homogeneous material, thus creating new opportunities for materials engineering employing controlled twin formation.

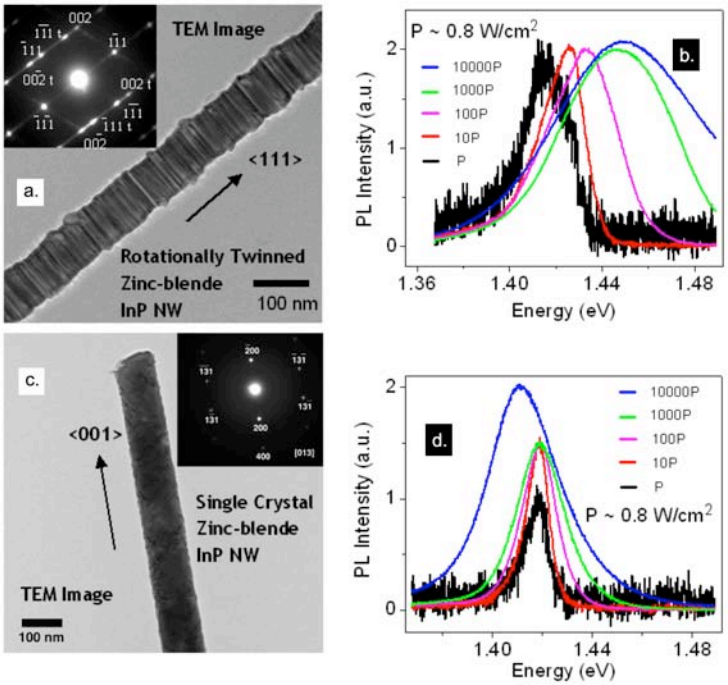

Figure 2.9. (**a**) TEM image of a RT InP nanowire. **Inset**: TEM diffraction pattern recorded along [110] zone axis. (**b**) PL of the nanowire in (a) under different excitation intensities at 7 K. The 488 nm laser was focused to a spot with ~2 mm diameter. The spectra are normalized to the same scale for ease of comparison. (**c**) TEM image of a single crystal ZB InP nanowire. **Inset**: TEM diffraction pattern recorded along the [013] zone axis, which reveals that the wire is single crystal (no twin planes) and the growth direction is <001>. (**d**) PL spectrum of the nanowire in (c) with different excitation intensities under the same conditions as in (b). The spectrum is scaled for ease of comparison.

Self-assembled Quantum Nanostructures

Pierre M. Petroff
Materials, University of California at Santa Barbara
***Collaborator(s)*:**

Research Goal. We are aiming at the development of a versatile nanostructure which allows for the manipulation of 3D confined electrons and holes and of their spins using optical pumping and band gap engineering. This nanostructure is the quantum post, which we started developing and studying last year.

Research Progress. In the last year, we have continued our work on a novel *self-assembled* quantum nanostructure: the quantum post (QP), which consists of a short quantum wire with a quantum dot at each end. We have developed a fair understanding of these structures and have demonstrated a unique exciton memory device, which can function as a source of single photon on demand. We also have demonstrated that giant dipole moments can be induced in the QPs and this may lead to new functionality in QPs devices.

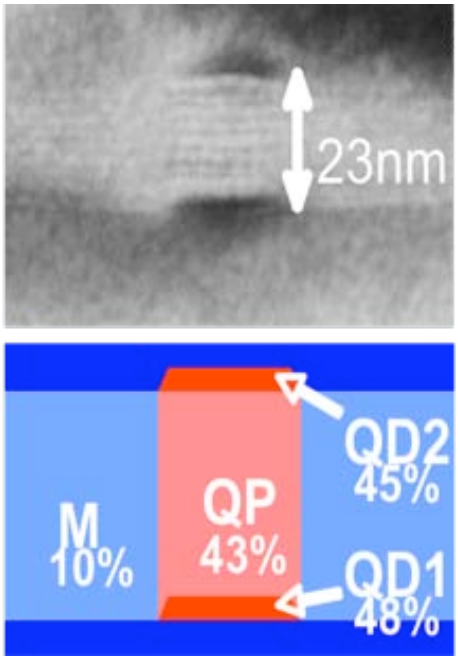

Figure 2.10. Schematic of a 23 nm high quantum post. The cross section TEM shows the stain fields associated with the top and bottom quantum dots. The schematic indicates the composition with the percentage of In in the $In_xGa_{1-x}As$ regions measured by EDX [ ]. The QP is grown by MBE on a GaAs substrate and the capping layer is GaAs.

The quantum post structure is shown in the schematic and the TEM cross section in Figure 1.

By integrating the QP structure in a p-i-n structure pumping optically with above band gap light, we are able to induce a giant dipole moments within the QPs. These are associated with the field-induced excitons dissociation and the localization of the electron and hole in the top and bottom QDs. The measured dipole values are obtained from the quantum confined Stark effect (QCSE) shift of the luminescence as a function of the applied field. Micro-photoluminescence spectra as a function of the applied field have been measured for QP with various height (16 nm – 40 nm). The characteristic transition of the QCSE into an asymptotically linear regime has been observed. The measured dipole P from the linear section varies as P ≈ H.e, where H is the QP height and e the electron charge. Thus we have a structure in which we can control the dipole strength electrically over a range of values, which is 2–3 orders of magnitude larger than that allowed with quantum dots. This effect is used in moving the delocalized electron and hole from one end of the QP to the other.

We have used the field-driven exciton dissociation for storing the exciton in individual and ensembles of QPs. Figure 2.11 shows the voltage sequence applied to the heterostructure to store excitons in an ensemble of QPs.

These data show long storage times (tens of milliseconds) and an expected voltage

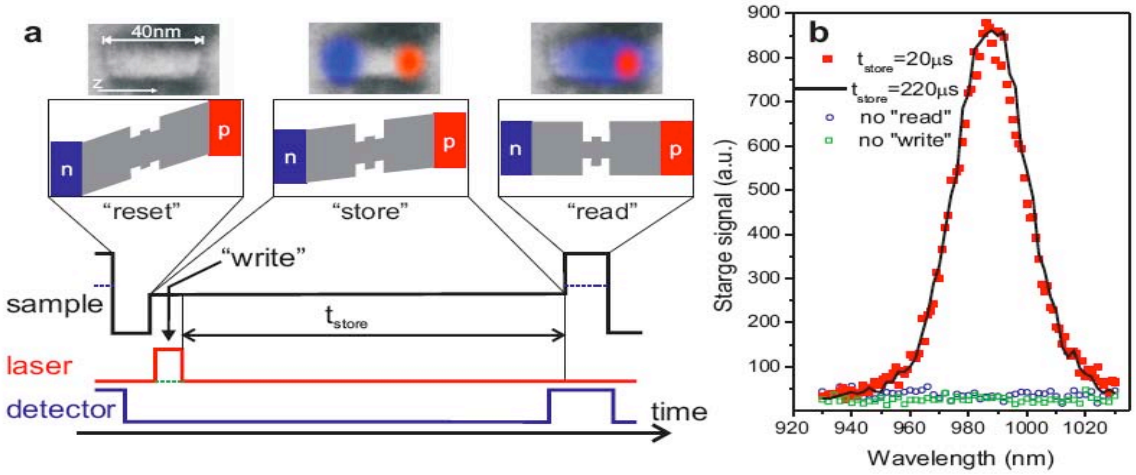

Figure 2.11. Storage of excitons in 40 nm high QPs. **(a)** Schematic of the storage scheme. After a reset step during which the QP is emptied the sample voltage (black) is switched to the indirect exciton regime. In the beginning of the storage interval electrons and holes are written by a laser (red) into the QP and after $t_{storage}$ read via direct excitons. The detection (blue) is activated only during the time of the read step. The band structure and spatial carrier distribution during each step are shown schematically. For control experiments the write and read pulses are turned off individually as shown by the dashed lines. **(b)** Spectra taken for 20 ms (full squares) and 200 ms (line) storage times (P_{exc} = 20 kW/cm^{-2}, T = 7 K). Without the "write" and "read" pulses (open symbols) no signal is detected as expected.

dependence of the storage time on the storage bias. This dependence is shown in Figure 2.12. The large storage bias will favor electron tunneling out of the QP and reduce the storage time.

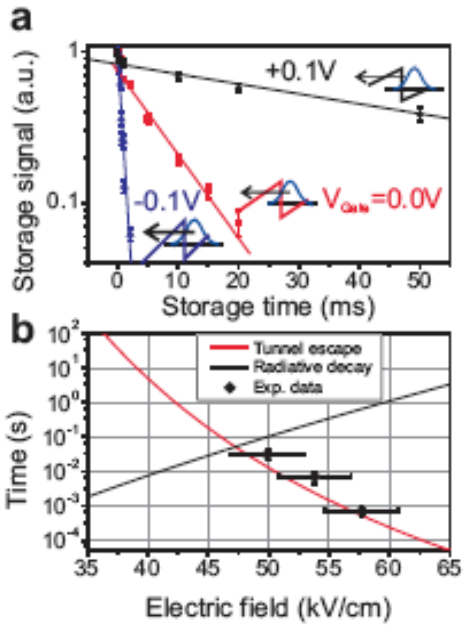

Figure 2.12. Temporal dependence of the storage signal. **(a)** For increasing reverse bias the storage signal decays over time due to tunnel escape of electrons from the QPs. **(b)** Comparison between experimentally observed decay times (symbols) and calculated tunneling times and radiative life times (red and black lines) as a function of the applied electric field F.

Microfabricated Water Immersion Zone Plate Optical Tweezer

Kenneth B. Crozier
Electrical Engineering, Harvard University
Collaborators: Mark Tuominen, Marc Ackermann (UMass, Amherst), James Hogle (Harvard Medical School); Jonathan Bernstein (Draper Labs.); Joyce Wong Schlumberger

Summary. We demonstrate the trapping of beads in water with a microfabricated Fresnel zone plate. Beads are loaded onto the microfabricated optical traps using conventional optical tweezers, and fluorescent microscopy is used to track bead position. Analysis of the bead position as a function of time is used to determine trapping stiffness. We present experiments showing the three-dimensional trapping of 2 μm diameter beads with trapping stiffnesses comparable to conventional optical tweezers, when the zone plate diffraction efficiency is taken into account.

Research Goal. The incorporation of optical tweezers into microfluidic chips would provide new functionalities for these systems, such as particle sorting, particle manipulation, and biophysical force measurements. Conventional optical tweezers use high numerical aperture microscope objectives to produce axial intensity gradients that are large enough to counter the scattering forces from small angle rays, enabling high trapping stiffness [1]. The short working distance (usually < 200 μm), size and cost of these lenses, however, make them impractical to integrate into microfluidic chips. This motivates the development of microfabricated structures for optical trapping that are suitable for integration into microfluidic chips.

Approach. In the past year, we have designed and demonstrated the use of a Fresnel zone plate to produce well-calibrated optical traps in an integrated system. The starting substrate is a glass slide coated with a thin layer of indium tin oxide (ITO) to prevent charging during lithography. Polymethylmethacrylate (PMMA) is spun on and exposed by e-beam lithography. Gold is evaporated to a thickness of 50 nm, with a thin layer of chrome used for adhesion. Lift-off is then performed, yielding the device shown in Figure 2.13(a). The light regions are gold and the dark regions are the glass areas where the gold has been removed. The zone plate is designed for use with a free space illumination wavelength of l = 976 nm, corresponding to a wavelength in water of l = 735 nm. The center of the zone plate is transparent and has a diameter of 6.46 μm. The performance of the zone plate is modeled with a two-dimensional split-step Fourier vector beam propagation (BP) algorithm [2]. Figure 2.14(b) shows a cross section of the intensity in a log scale at the focal plane for **y** polarized incident light. The focal spot size has a full width at half maximum (FWHM) of 303 nm in the x-axis and 470 nm in the y-axis. Figure 1(c) shows a y-axis cross section of the intensity through the beam focus, which yields an axial FWHM of 758 nm along the z-axis. Around the focal region there are numerous sidelobe peaks, but their peak intensity is less than 1/10 of the intensity of the central peak. The gold is modeled as an opaque region where the transmission coefficient is 0.1.

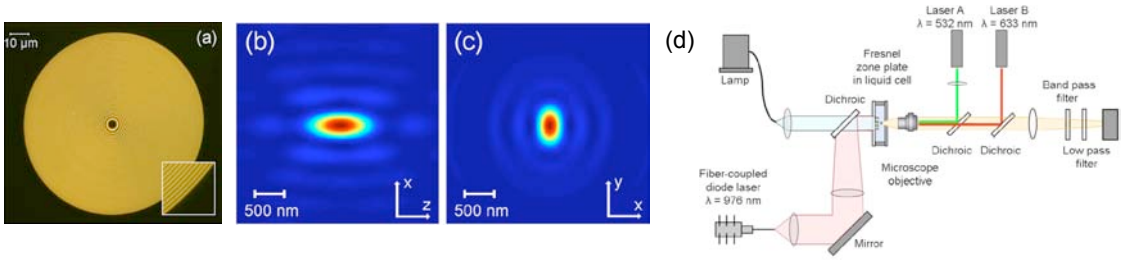

Figure 2.13. (**a**) Photo of fabricated Fresnel Zone Plate. (**b**) Simulated axial *x*-*z* plane intensity distribution of the focal spot. (**c**). Cross section *x*-*y* plane of the transverse intensity at the focus 8 mm behind the zone plate. (**d**) Schematic of Fresnel zone plate optical tweezer experimental setup.

The experimental set-up (Fig. 2.13d) is used to characterize the trapping performance. Light from a fiber-coupled diode laser (l_0 = 976 nm) is collimated and focused onto the zone plate chip using a 200 μm focal length lens. This produces a spot with a diameter of 180 μm that overfills the 100 μm diameter of the zone plate. A liquid cell is formed by sandwiching a layer of water between the zone plate chip and a coverslip. Fluorescent beads with diameters of 2 μm are trapped at the zone plate focus. A green laser (l_0 = 532 nm) is used to excite fluorescent emission from the trapped beads, which are imaged by a microscope objective onto a CCD camera. A HeNe laser trap is used to load beads into the zone plate trap. A bandpass filter and dichroic mirrors are used to block the trapping, green and HeNe lasers, so that only the fluorescent emission is collected onto the CCD camera. A tungsten lamp is used for white light illumination.

Results and Accomplishments. Figure 2.14(a) shows a polystyrene bead (2 μm diameter) trapped by the zone plate. In this CCD image, both the green laser and the lamp are on. The central rings of the zone plate are visible, although out of focus due to the fact that they are 8 μm behind the bead. In order to determine the trapping stiffness, movies of trapped beads are acquired at video rate to capture the bead motion as a function of time. Centroid calculations are performed on the images to monitor the bead position.

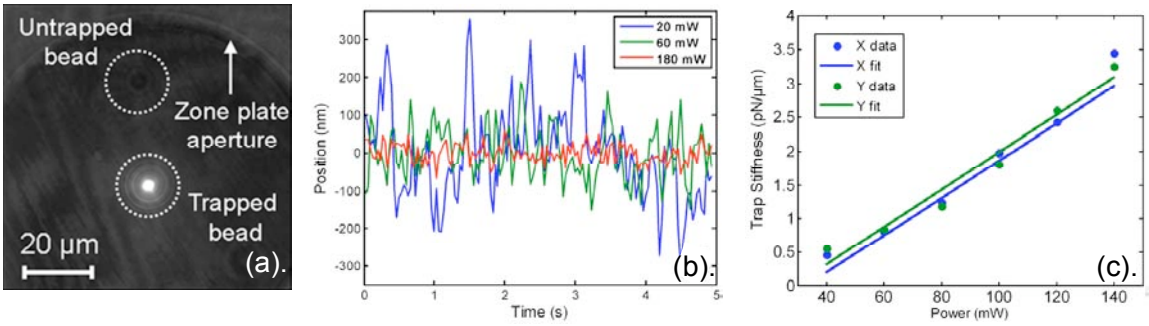

Figure 2.14. (**a**) CCD Image of 2 μm bead trapped by Fresnel Zone Plate. (**b**) Bead position along *x*-axis as a function of time for different laser powers. (**c**) Trap stiffness k_{trap} along *x* and *y* axes as a function of laser power.

Figure 2.14(b) shows three traces of the bead position for laser powers of 20, 60, and 180 mW. As expected, the variance of the bead position is approximately inversely proportional to laser power. The measured trap stiffness, with motion blur corrected for, is plotted in Figure 2.14(c) as a function of laser power. A linear fit of the curves shows that the power-normalized stiffness is 0.0279 pN/μm·mW along the *x*-axis and 0.0245

pN/μm·mW along the *y*-axis. At the highest laser powers, the stiffness deviates from the linear fit. We believe this is due to the generation of convection currents in the trap at these power levels that tend to destabilize the trap. Overfilling the zone plate aperture reduces the trap intensity by a factor of four, which then gives the zone plate trap a stiffness of one tenth of the theoretical optimum of 1 pN/μm·mW [3,4] for a 2 μm polystyrene sphere. This factor of ten can be traced to the diffraction efficiency of a binary amplitude grating, which is $1/\pi^2$ [2]. By using a π phase zone plate, the stiffness could be increased by an additional factor of 4. Even at the zone plate's current stiffness value, it compares well to high performance traps which frequently have values of 0.1 pN/μm·mW [5].

The focusing optic is the single most important element in an optical trap [5], and we have presented a substantial modification to the traditional experiment. Considerable flexibility can be added to optical tweezer experiments by taking advantage of a zone plate's much smaller cross section, thickness, and weight. Optical traps can be embedded deep inside fluidic chambers without the limitation of an immersion objective's small working distance. In addition, the fact that the trapping is decoupled from imaging, allows traps to be translated, with the trapped particles remaining fixed relative to them. We have experimentally shown that zone plate optical tweezers have comparable stiffness to traditional optical tweezers, and because of the flexibility of the lithographic process, this element can be further designed to implement functions that objective lenses cannot.

References

[1] M. Lang and S.M Block, *Am. J. Phys*. **71**, 201 (2003).
[2] J.W. Goodman, *Introduction to Fourier Optics* (McGraw-Hill, New York, 1996).
[3] A. Rohrbach, *Phys. Rev. Lett*. **95**, 168102 (2005).
[4] N. B. Viana, A. Mazolli, P. A. Maia Neto, H. M. Nuessenzveig, M. S. Rocha, and O. N. Mesquita, *Appl. Phys. Lett.* **88**, 131110 (2006).
[5] K. C. Neuman and S. M. Block, *Rev. Sci. Instrum*. **75**, 2787 (2004).

Silica Nanowires for Microphotonic Devices

Eric Mazur
Applied Physics and Physics, Harvard University

Research Goal, Approach and Accomplishments: Silica nanowires provide strong mode confinement in a simple cylindrical silica-core/air-cladding geometry, representing a model system for the study of the nonlinear propagation of short pulses inside fibers. We observed supercontinuum generation by femtosecond laser pulses in silica fiber tapers of minimum diameters as small as 90 nm. This research was presented at the Photonics West 2006 Conference and was published in *Optics Express* **14**, 9408–9414 (2006).

Supercontinuum generation refers to extreme spectral broadening of a laser pulse propagating in a nonlinear material. The figure above shows the visual and spectral evidence of supercontinuum generation. Qualitatively, the degree of broadening of the supercontinuum spectra is understood in terms of the diameter-dependent dispersion and nonlinearity of the fiber. Contrary to supercontinuum generation by nanosecond pulses, for laser pulses propagating in negative dispersion regime, the observed spectrum is consistent with higher-order soliton formation and break-up. Because of the reduction of the interaction length to ~20 mm, and the low energy thresholds supercontinuum generation in tapered fibers is a viable solution for coherent white-light source in nanophotonics. Additionally, sub-200-nm diameter fibers possess negligible dispersion and nonlinearity making these fibers ideal media for propagation of intense, short pulses with minimal distortion.

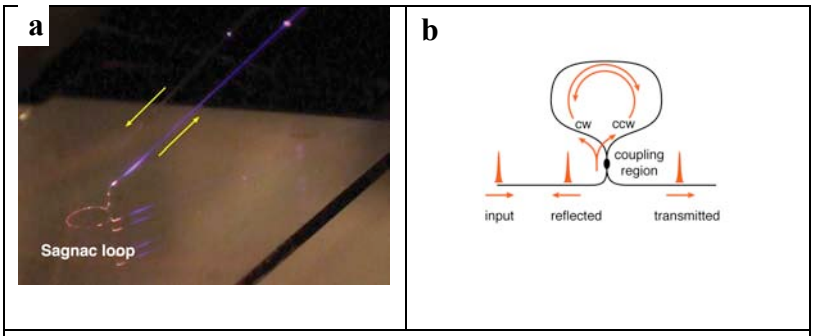

Figure 2.15. (a) Photograph and **(b)** diagram of a nonlinear Sagnac interferometer fabricated from silica nanowires showing the input pulse, the counter-propagating paths, the reflected and transmitted pulses.

The low threshold energies required to generate supercontinuum indicate that microphotonic devices can be constructed that take advantage of these nonlinear effects. We also present a device based on the nonlinear Sagnac interferometer that permits optical switching and a number of all-optical logic operations with femtosecond laser

pulses in the nanojoule range. The spectral broadening studied in the supercontinuum experiment reveals an optimal fiber diameter to enhance nonlinear effects with minimal dispersion. We fabricate Sagnac loops with lengths of about one millimeter from silica nanowires with diameters of 500–800 nm, as shown in the figure. Preliminary results show that we achieve light-on-light modulation. The data show excellent agreement with predicted transmission behavior for a nonlinear Sagnac interferometer with a coupling parameter of 0.08. Our current research efforts are to increase the modulation depth of the transmission by controlling the coupling, and to significantly reduce the interaction length required for nonlinear phenomena.

Silica nanowires have also been used to efficiently launch light into ZnO nanowires. The optical properties of semiconductor nanowires are often characterized by using side-illumination. We can directly access the waveguide modes of the semiconducting nanowires by injecting light from tapered silica fibers. Initial results were presented at the Photonics West 2007 Conference and this work was published in *Nano Letters* **7** (12), 3675–3680 (2007).

Electronic Properties of 1-atom Layer MX_n Structures

Cynthia M. Friend
Chemistry and Applied Physics, Harvard University

During the past year, we have investigated the synthesis and properties of 2-D nanostructures—materials that are 1 atom layer thick. We have completed our studies of metal oxides, e.g., MoO_3, and investigated the electronic and geometric properties of specific types of defects om the nanostructures. To this end, we have also developed methods for introducing vacancies in a controlled manner and subsequently investigating the electronic structure of these materials using density functional theory. We have also studied the formation of 1-atom high layers of, e.g., AuCl, in order to understand bonding and stability in the structures of small scale materials.

In previous NSEC work, we focused on the synthesis of 2-D metal sulfide and metal oxide nanostructures on Au. The Friend group has already developed a synthetic method for making 2-D metal sulfide nanostructures with well-defined crystalline structure, composition, and morphology. For example, crystalline nanostructures of TiS_2 and MoO_3 were synthesized on a Au substrate and imaged using STM [1, 2] .

We subsequently developed methods for controlled thermal reduction of these materials that introduce specific types of vacancies. Both MoO_{3-x} and TiS_{2-y} have been created by synthetic methods developed in our group. In both cases, the nanostructures remain only 1 atom high; however, there are reduced regions of the surface that manifest themselves as shear lines in the STM images (Fig. 2.16). Density functional theory was

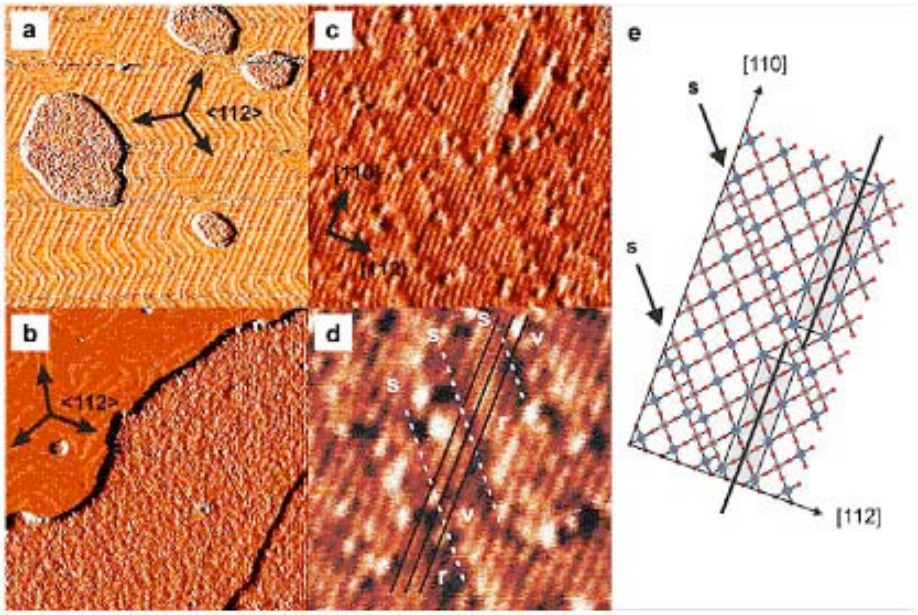

Figure 2.16. Scanning tunneling microscope image of (**a**) stoichiometric 1-atom-layer-high MoO_3 nanostructures synthesized on Au(111) and **(b–d)** reduced MoO_x nanostructures containing a mixture of Mo^V and Mo^{VI} showing 1-D shear lines in the material at various magnifications. A schematic model of the 1-D defect structure is shown on the right **(e)**. The electronic properties were also modeled using theoretical (density functional) methods. The scales for the images are **(a)** 125 x 125 nm, **(b)** 85 x 85 nm, **(c)** 17 x 17 nm, and **(d)** 8 x 8 nm. The images shown were obtained with the CNS Omicron STM.

used to study the electronic properties of the MoO_{3-x} and to determine the atomic-scale structure. The electronic properties of the 1-atom high layer is different than the bulk—it is semimetallic. Furthermore, the Mo along the shear lines have a lower oxidation state, indicating that electron transport and chemical reactivity will be different in these regions of the material [3].

In our more recent work, we have investigated the formation of 1-atom high metal complexes of other electronegative elements [4]. Our work to date has focused on Au because of its widespread use in soft lithography and because it was used as a substrate in our earlier synthetic work. Importantly, our studies have shown that surface atoms are readily incorporated into a 1-atom high layer via reactive processes. This is a key result becacuse it shows that stablizing the structure of nanoscale objects is difficult in a reactive environment. In the specific example of Cl on Au has been particularly interesting because our combination of experimental imaging studies and theoretical investigations using density functional theory show that the bonding in this atomic layer is mainly covalent (as opposed to ionic), contrary to conventional wisdom. These results have a profound influence on the charge distribution in Au nanostructures, which will affect electronic and chemical properties. (Fig. 2.17).

In our future work, we propose to synthesize transition metal oxides and metal sulfides on nanoporous Au [5,6] in order to study their optical properties. We are particularly interested in the ability to efficiently couple visible and ultraviolet light to these materials for the potential purpose of creating new substrates for photochemistry and for anchoring and spectroscopically probing biomolecules.

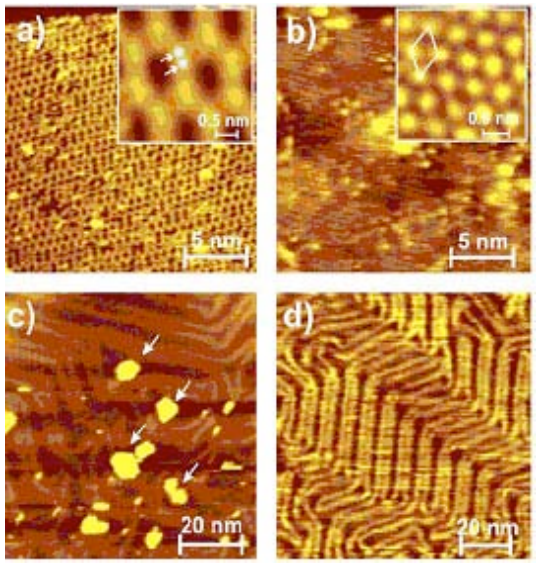

Figure 2.17. Scanning tunneling microscope images of chlorine atoms on Au illustrate the importance of the chemical environment on the ability to form and retain the structure of nanostructures. Chlorine atoms form a structure that lifts Au out of the bulk at high Cl concentrations (~0.8 Cl atoms per Au surface atom) (*top left panel*, **a**). As the surface is heated, Cl leaves the surface and intermediate structures are formed that illustrates the release of Au atoms. Panel **c** (*lower left*) clearly shows nanoscopic Au islands. When all Cl is removed, the surface reverts to the characterisitic "herringbone" structure (*lower right panel*, **d**). We have also performed theoretical calculations on these systems to develop an understanding of the energetic factors in determining the structures formed. These data are reproduced from W.W. Gao *et al*., *J. Am. Chem. Soc*., in press (2008).

References

[1] Biener, M.M., J. Biener, R. Schalek, and C.M. Friend, *J. Chem. Phys.* **121** (23), 12010–12016 (2004).
[2] Biener, M.M., J. Biener, and C.M. Friend, *J. Chem. Phys.* **122** (3), article #: 034706 (2005).
[3] Deng, X., J. Biener, M.M. Biener, S.Y. Quek, C.M. Friend, and E. Kaxiras, *Surf. Sci.,* in press (2008).
[4] Gao, W., T.A. Baker, L. Zhou, E. Kaxiras, and C.M. Friend*, J. Am. Chem. Soc*, in press (2008).
[5] Biener, J., A.M. Hodge, J.R. Hayes, C.A. Volkert, L.A. Zepeda-Ruiz, A.V. Hamza, and F.F. Abraham, *Nano Lett.* **6** (10), 2379–2382 (2006).
[6] Kucheyev, S.O., J.R. Hayes, J. Biener, T. Huser, C.E. Talley, and A.V. Hamza, *Appl. Phys. Lett.* **89** (5), (2006).

Semiconductor Heterostructures for Nanoscale Devices

Arthur C. Gossard
Materials University of California at Santa Barbara
Collaborators: Marc A. Kastner (MIT); Venkatesh Naraynamurti, Charles M. Marcus, Robert M. Westervelt (Harvard University)

Research Goal, Approach and Accomplishments. The primary goal of Gossard's NSEC research at UCSB was to develop molecular beam epitaxy-grown semiconductor quantum structures for use in NSEC investigations. This work concentrated on growing materials for fabrication into quiet, stable gated quantum devices at Harvard and MIT Materials were grown for the imaging of electron flow in semiconductor structures (by the **Westervelt** group), noise correlations of charges in single and coupled quantum dots and quantum point contacts (with the **Marcus** group), and energy- and spin-dependent electron tunneling and spin relaxation in quantum dots (with the **Kastner** MIT group). We also grew materials for probing energy barriers and quantum states in semiconductor heterostructures (with the **Narayanamurti** group).

Our approach for imaging electron flow and for materials for coupled quantum dots and quantum contacts was to grow high mobility modulation-doped two-dimensional electron gas structures containing electron gases near the surface of the samples. For the probing of energy barriers and states in heterostructures, we grew sets of both indium arsenide quantum dot samples and gallium arsenide/aluminum arsenide based heterostructures of varied composition and dimensions.

This work resulted in the publication of five *Physical Review Letters*, one *Physical Review* article, one *Applied Physics Letter* and one *Nature Physics* paper with our NSEC collaborators during the year and the submission of two more papers that are currently under review and another that is in preparation.

Electronic and Structural Properties of High-quality VO_2 Thin Films

Shriram Ramanathan
Chemistry, Physics, Harvard University
Collaborator: Venkatesh Narayanamurti (Harvard University)

Research Goal, Approach and Accomplishments. Research goal was to synthesize high-quality vanadium oxide thin films and investigate their structural and transport properties. Further, our goal was to fabricate microfabricated devices and study phase transition phenomena.

Motivation and Goals. There is a critical need for innovative approaches to enable continued scaling of nanoelectronic devices, in particular those that do not suffer from limitations of existing complementary metal-oxide-semiconductor (CMOS) devices. Revolutionary solutions incorporating novel materials and device concepts are therefore essential to enable continued scaling particularly for the 2019+ timeframe and also overcome constraints from simple geometrical lateral scaling of devices. Phase transitions in nanoscale complex oxides are exciting phenomena that can have relevance to device technologies, particularly to fabricate nanoscale switches and memory elements. Our goals is to investigate transport phenomena in vanadium oxide thin films that undergo a metal-insulator transition accompanied by dramatic changes in electrical and optical properties across the phase transition. Potential outcome of our research could be enabling a novel switch utilizing phase transitions.

Research Accomplishments. Ramanathan and group members have successfully demonstrated phase transitions in vanadium oxide thin films synthesized by vapor deposition methods. Figure 2.18 shows conductance transition of ~ *5 orders magnitude* in a VO_2 film. Further, recently, they have demonstrated that origin of the phase transition can be mapped to changes in electronic structure as seen by X-ray absorption spectroscopy. Figure 2.19 shows the O-K edge signature of metallic and insulating states studied by *in situ* X-ray absorption spectroscopy. Figure 2.20 shows recent data from ongoing work on electric field-induced conductance change in VO_2 films. Although the field effect is modest at this point, the researchers are planning to achieve more dramatic changes through a shorter channel length and an improved gate dielectric. Figures 2.21a-c provide some more details into the optical reflectance changes that accompany the metal-insulator transition as well as tuning the resistance of the oxide films at low temperatures utilizing photon radiation. This is a powerful approach to modulate the resistance of a functional oxide film with silicon processing compatible temperatures.

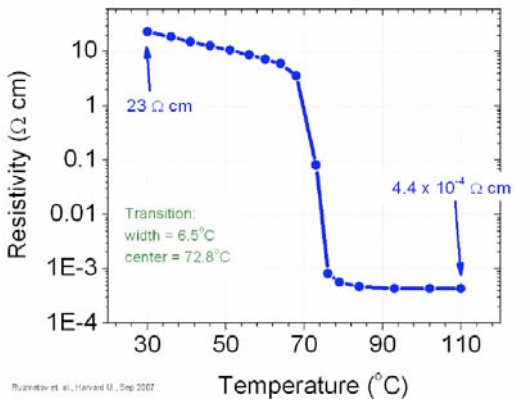

Figure 2.18. Metal-insulator transition in VO_2 film with *10^5 change in resistance.* The film was grown in PI's lab at Harvard.

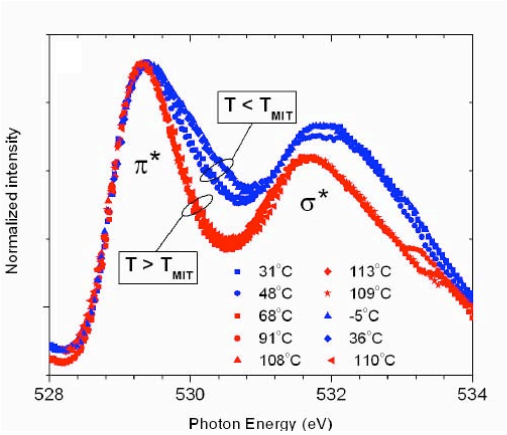

Figure 2.19. O-K near edge fine structure mapped for metallic and insulating states using *in-situ* NEXAFS.

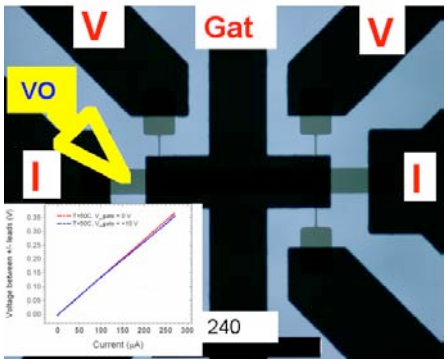

Figure 2.20. Micrograph of a three-terminal switching device fabricated at Harvard and inset shows preliminary data of electric field-induced channel resistance change.

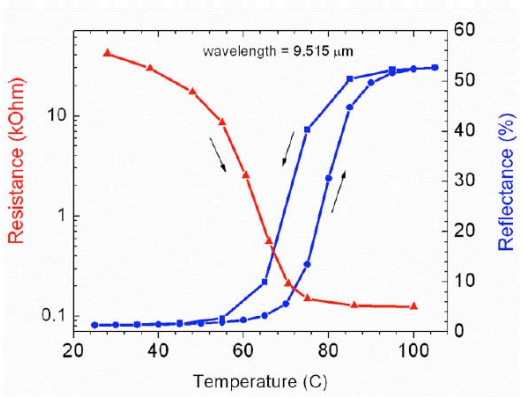

Figure 2.21a. Dramatic changes in optical reflectance accompany the metal-insulator transition in VO_2 films.

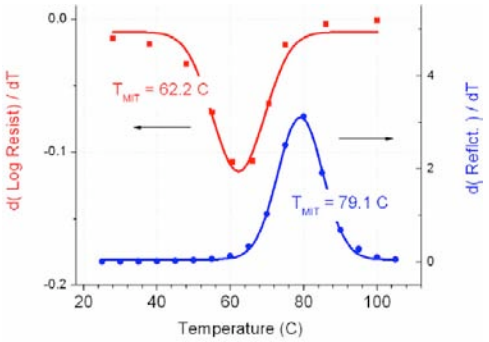

Figure 2.21b. Shift in the electrical and optical reflectance observed may hold insights into mechanisms governing the electronic phase transition.

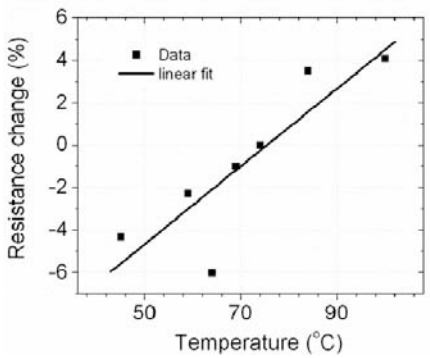

Figure 2.21c. Dynamic tuning of resistance utilizing photon radiation in VO_2 films demonstrated in Park's lab.